Novel bioelectrochemical strategies for domesticating the electron flow in constructed wetlands

Amanda Prado de Nicolás [a,b,*], Carlos A. Ramírez-Vargas [c,d], Carlos A. Arias [c,d], Abraham Esteve-Núñez [a,b,*]

[a] Chemical Engineering Department, Universidad de Alcalá, Alcalá de Henares, Spain

[b] IMDEA Agua, Parque Tecnológico de la Universidad de Alcalá, 28805, Alcalá de Henares, Spain

[c] Department of Bioscience, Aarhus University, Ole Worms Allé 1, 8000 Aarhus C, Denmark

[d] WATEC, Aarhus University, Ny Munkegade 120, 8000 Aarhus C, Denmark

GRAPHICAL ABSTRACT

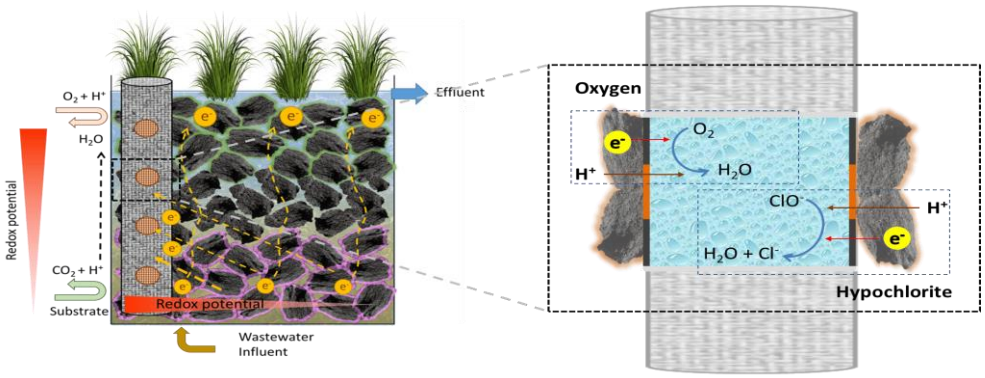

* Corresponding authors at: Bioe Group, Chemical Engineering Department, Universidad de Alcalá, Madrid, Spain.

E-mail addresses: amanda.prado@imdea.org (A. Prado de Nicolás), abraham.esteve@uah.es (A. Esteve-Núñez).

Abstract: Constructed wetlands are an effective biofilter-based technology for treating wastewater in a sustainable way; however, their main disadvantage is a large area footprint. To cope with this limitation a new generation of constructed wetlands, the METlands®, have been recently reported. METlands® replace gravel with a granular electrically conductive material to enhance the oxidative metabolisms of electroactive bacteria by facilitating the flux of electron through the material and, consequently, increase bioremediation rates. In this work we evaluated the performance of a new electron sink (e-sink) device with the purpose of controlling and enhancing the electrochemical consumption of electrons from microbial metabolism without energy consumption. The e-sink device was integrated inside the biofilter bed and was tested using different electron acceptors with high redox potentials, like oxygen and hypochlorite. Interestingly, the presence of the e-sink allowed novel redox gradients to form inside the METland® and, consequently, a new electron flow was demonstrated by measuring both the electric potential and current density profiles of the bed. Three

independent biofilters were constructed and operated under flooded conditions. Ec-coke and electroconductive biochar (ec-biochar) were used as electrically conductive bed materials, while gravel was used as an inert control. Furthermore, e-sink integration inside the electrically conductive bed outperformed METlands® for removing pollutants, already much more efficient than standard gravel biofilters. COD removal was increased from 90% in METland® to 95% in the e-sink METland® as compared to 75% for the control, while total nitrogen removal was enhanced from 64% in METland® to 71% in e-sink METland® as compared to 55% for the control. Our results indicate that increasing the electrochemical availability of electron acceptors by using the e-sink will be a suitable method for controlling the electron flow inside the filter bed and can be integrated in full scale METlands® for achieving high removal rates.

Keywords: constructed wetland, METland®, microbial electrochemical technologies, electroactive bacteria, ec-biochar.

1. Introduction

Constructed wetlands (CW) are biological wastewater treatment systems that mimic the physical, chemical, and biological degradation processes taking place in natural wetlands. This technology emerged several decades ago (Brix, 1994) as a robust, eco-friendly, and cost-effective decentralized treatment system that requires low operational and maintenance costs (Brix et al., 2007; Dotro et al., 2017; Vymazal, 2008; H. Wu et al., 2014). CWs can be used to treat a wide range of water pollutants such as domestic wastewater (García et al., 2010), industrial wastewater (Vymazal, 2014), mine drainage (Isosaari P. & Sillanpää M. , 2016), agricultural runoff (Roley et al., 2012) and urban storm runoff (Carleton et al., 2000). However, when compared to conventional biological wastewater treatments CW's main disadvantages are the large footprint of land required and certain limitations for nutrient removal (Kadlec and Wallace, 2009).

Therefore, to reduce the surface area requirements, constructed wetlands have been evolving from passive into intensified systems (Wu S. et al., 2014) by supplying oxygen to enhance oxidative metabolism. More recently, the new-born discipline of microbial electrochemistry has been applied to constructed wetlands in the name of intensification (Ramírez-Vargas et al., 2018)). Redox gradient profiles along the depth of a CW are produced as it transitions from aerobic zones at the top to anoxic zones at the bottom. This scenario lends to the application of a microbial electrochemical system where pollutants can be converted into electrical current by the metabolic activity of the electroactive bacteria and form a new gradient to increase removal efficiency (Corbella et al., 2014; Aguirre-Sierra et al., 2016; Wang et al., 2017).

The integration of microbial electrochemical technologies (MET) into constructed wetlands is illustrated by the many different configurations used (Ramírez-Vargas et al., 2018). The microbial fuel cell (MFC) is able to harvest energy from the wetland using an anode located in the anaerobic zone (bottom) and a cathode located in the aerobic zone (top). These are separated by a layer of inert material (gravel) and connected through an external circuit (Zhao et al., 2013; Corbella et al., 2014). Microbial electrolysis cells (MEC) are integrated into the wetland in a similar manner as the MFC but the electrodes are polarized through a potentiostat or a power source (Aguirre-Sierra et al., 2016; Srivastava et al., 2018). Microbial electrochemical snorkels (MES) are the most basic

configuration, simply a conductive bed that forms a redox gradient according to the chemical environment around the material. Anodic and cathodic reactions are not occurring under different electrodes but in different locations of a unique conductive body. This situation is ideal when the objective is to raise electrochemical reaction rates that do not require a strict control of redox potential. In contrast with standard two-electrode systems, the microbial metabolism cannot be converted into electric power (Aguirre-Sierra et al., 2016; Ramírez-Vargas et al., 2019) (Fig. 1S). Despite their good performance at the laboratory scale, full scale implementation of the CW-MFC is under development due to a number of challenges. Mainly, internal resistance in the CW–MFC is dependent on both the resistance of the electrolyte and the material-based electrical resistance between the electrodes. This resistance increases linearly as the size and distance between electrodes increases (Doherty et al., 2015).

The METland® (Aguirre-Sierra et al., 2016) is an alternative configuration based on a continuous bed of electrically conductive material, also known as a MES. This material promotes the metabolism of electroactive bacteria by acting as an inexhaustible connector with the distant terminal electron acceptors (TEAs), like surface oxygen. The concept has been successfully tested under flooded conditions such as those found in conventional horizontal subsurface flow (HSSF) wetlands (Aguirre-Sierra et al., 2016; Prado et al., 2019; Ramírez-Vargas et al., 2019) COD removal rates were as high as 400 g/m3day with real urban wastewater fed at ca. 0.5 m3/m2day (Aguirre-Sierra, 2017). Interestingly, the system outperformed classical gravel-based HSSF CW reaching a ratio of 0.4 m2/pe. The METland® can also outperform conventional CW in their ability to remove emergent pollutants in the form of pharmaceuticals (Pun et al., 2019). Many different carbon-based electroconductive materials have been tested for use in the METland® system (Aguirre-Sierra et al., 2016; Ramírez-Vargas et al., 2019), electrically conductive biochar, from the high-temperature pyrolysis of various Quercus biomass, showed the best performance (Prado et al., 2019; Schievano et al., 2019).

Unlike typical bioelectrochemical systems, METlands® do not have two differentiated electrodes but host anodic and cathodic reactions on the surface of a single electrode bed exposed to different redox environments. Thus, in METlands® the major anodic and cathodic processes follow a gradient across the depth of the bed. The main cathodic process, like the reduction of oxygen, happen at the

upper bed layers whereas the anodic oxidation of organic matter occurs in the anoxic bottom layers; (Ramírez-Vargas et al., 2018). The vertical separation of the anodic and cathodic reactions promotes a local charge imbalance that generates an electric field and an increased electric potential with depth. The electric field can be used to estimate the electric current generated by the electroactive bacteria, a method already followed to measure the electric current generated by cable bacteria in marine sediments (Risgaard-Petersen et al., 2014).

In this context, the electron flow generated inside METland® systems are a direct consequence of the electroactive bacteria's metabolism. They use a mechanism similar to the one reported in natural electric current generators like geobatteries or biogeobatteries (Nielsen and Risgaard-Petersen, 2014), in which a conductive material crosses two different redox domains, like that found in the transition between sediment and the water column in a pond or lake. The electrically conductive material allows the transport of electrons from the anodic oxidation reactions in the sediment to the cathodic reduction reactions near the water's surface (Nielsen et al., 2010). Furthermore the sediment acts as an electrolytic conductor allowing ion migration to complete the electric circuit and maintain charge balance (Sato and Mooney, 1960). Interestingly, ion migration in the METland® is taking place in the pore water and generates a typical electric potential profile that is absent in gravel-based CW (Ramírez-Vargas et al., 2019). The long-distance separation (30-40 cm) between cathodic and anodic processes by electrically conductive material represents a change in the paradigm of biological wastewater treatment where the conventional thinking was that both electron donors and acceptors for a metabolic process need to be in the same living cell, or at least within a few micrometers of each other. In METlands®, bacteria can directly use electrically conductive material as an electron mediator, these electrons can flux to cathodic areas where TEAs, such as oxygen or nitrate, can be reduced to further drive the formation of a redox gradient.

Unlike most MET applications which require an anaerobic environment, METlands® can operate as an aerobic vertical subsurface downflow (VSSF) biofilter (Aguirre-Sierra et al., 2020). The presence of oxygen enhances nitrifying conditions over gravel-based systems and unexpectedly it promoted the presence of electroactive bacteria from *Geobacter* genus typical of anoxic environments (Aguirre-Sierra et al., 2020). Thus, operational modes in METland® allow for additional control of redox gradients and electron transfer along bed, this is nearly impossible in standard CWs.

123 This work aims to integrate the new concept of the e-sink into METlands® to artificially create new
124 redox gradients to promote both electron transfer and biodegradation of pollutants in wastewater.
125 This novel device will allow for the "domestication" of the flux of electrons from microbial metabolism
126 and allowing for their distal consumption in environments different from their original biological niche.

127 ## 2. Materials and Methods

128 ### *2.1 Construction of the e-sink device*

129 The electron sink (e-sink) device was built using electrically conductive carbon fiber tube (20 cm
130 long x 2 cm diameter) sealed at the bottom with a silicone stopper. This created a cylindrical chamber
131 capable of housing a solution. The tube was further drilled to produce 0.5 cm holes every two
132 centimeters (Fig. 1). All holes where sealed with a cation exchange membrane (Nafion®) to keep the
133 tube impermeable to water but allowing for the flow of protons into the interior of the e-sink. Direct
134 contact with the bed granules allows for a flux of electrons passed through the carbon fiber tube and
135 interact with the solution inside the e-sink. The e-sink devices were installed inside beds of either
136 gravel, ec-coke, or ec-biochar and different catholytes were tested in the e-sink (Fig. 2S):

137 i) Oxygenated water $O_2 + 4e^- + 4H^+ \rightarrow 2H_2O$

138 ii) Hypochlorite 80 mM solution $HClO + 2e^- + H^+ \rightarrow Cl^- + H_2O$

139 ### *2.2 Biofilters construction and operation*

140 Three biofilters were built with three bed materials: ec-coke (C), ec-biochar (ecB) and gravel (G).
141 The ec-coke and ec-biochar are electrically conductive and carbonaceous while the third, gravel,
142 was an inert control (Table 1). Each biofilter consisted of a 5.4 L polyvinylchloride (PVC) cylinder
143 (diameter: 25 cm, height: 15 cm), with an outlet at a height of 11 cm to maintain the water level, and
144 a perforated pipe inlet in the bottom of the system. Each biofilter was filled with the materials
145 previously stated, the pore volume was approximately 50% of total volume.
146 An e-sink device was placed next to the inner wall of each biofilter. In addition, three perforated
147 pipes for sampling were placed inside the biofilter at different distances (0, 6, 12 cm) from the e-sink
148 device (Fig. 1), these pipes were the sample points SP1, SP2, and SP3 respectively.

Table 1. Physiochemical characteristics of bed materials.

	EC- Coke (C)	EC-Biochar (ecB)	Gravel (G)
Density [g/cm^3]	0.5	0.5	0,6
Resistance [Ω]	1	15	-
Porosity [%]	48	52	43
Granulometry [cm]	1.5-3	2-3	1.5-3

The biofilters were housed outdoors with natural temperature variations (ranging from 13ºC to 34ºC) but protected from rain. The systems were fed with urban wastewater containing 625 mg/L COD, 320 mg/L BOD_5, 45 mg/L total nitrogen (TN). The columns were operated in a continuous up-flow mode with a hydraulic loading rate of 0.6 L/d and COD loading rate 88 g COD/m^{3}d for 45 days, using a peristaltic pump (LongerPump®).

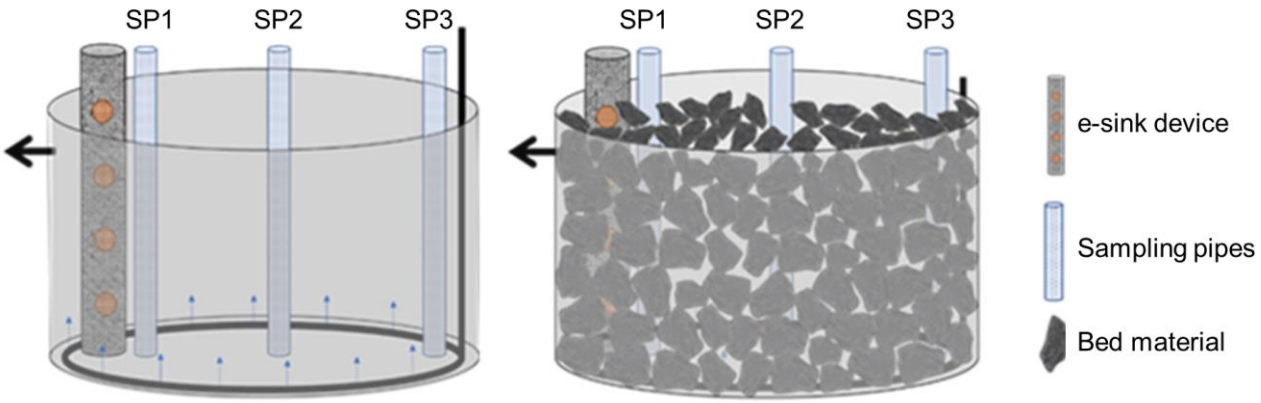

Fig. 1. Biofilter scheme without (left) and with (right) bed material.

2.3. Sampling and laboratory analysis

Steady state conditions for the biofilters were reached after three weeks of an initial acclimation period. Steady state was defined as constant removal efficiencies for each of the biofilters. Then, to study the COD and nutrient removal efficiency, three conditions were tested based on the electron acceptor used in the e-sink device: (1) control: empty e-sink device, so removal efficiency was just depending on the bed material, (2) oxygen saturated water, and (3) an 80mM hypochlorite solution. Each condition was operated for a week before sampling. For each experimental condition three samples were taken. The samples were taken every 48 h.

Influent and effluent samples were analyzed for the presence of COD, and N species. COD analysis was carried out by photometric evaluation (Hach LCK cuvette test + DR 3900 spectrophotometer).

BOD_5 analysis was performed using respirometric method (WTW OxiTOP®). NH_4^+ and NO_3^- was measured with photometric evaluation (Hach APC and LCK cuvette test + DR 3900 spectrophotometer).

2.4 Electric potential measurements

To measure the electric potential (EP), a custom-made shielded silver/silver chloride EP sensor was developed (height: 60 cm; diameter: 0.12 cm) (Ramírez-Vargas et al., 2019). These EP electrodes were built to be insensitive to redox-active compounds (Damgaard et al., 2014). The EP sensor was coupled to an Ag/AgCl reference electrode placed on the surface of the biofilter below the surface water. Both electrodes were connected to a digital voltmeter. The electric potential was measured in each sample point (SP1, SP2, SP3) in steps of 1cm against Ag/AgCl reference electrode positioned in the top water column. Profiles were measured to 11 cm depth in the biofilters (Fig. 3S). Each profile point was measured for 30 sec, recording one data point per second. For all profiles, the signal value in the overlying water was subtracted from all the values in the profile, resulting in profiles of electric potential relative to that of the overlying water, which was used as a reference potential for normalized the EP values.

The METland® represents a complete electric circuit in which charges are carried as i) electron currents within the electrically conductive material and ii) as ionic currents in the pore water. At steady state, these currents are equal in magnitude but opposite in direction (Sato and Mooney, 1960). The ion current density running through the bed obeys Ohm's law (Risgaard-Petersen et al., 2014) can, consequently. be quantified from the EP and the conductivity of the water *(σ)*, which, with a homogenous distribution of electroactive bacteria, implies that the quantity of electrons running in the biofilter bed per second through a unit area, i.e., the electron current density *(J)*, can be estimated as (Risgaard-Petersen et al., 2014):

$$J = -\sigma \cdot \frac{d\varphi}{dz} \qquad (Eq.1)$$

Where J [A m^{-2}] is the electron current density, σ [S m^{-1}] is the electrical conductivity of water in the column and $\frac{d\varphi}{dz}$ [V m^{-1}] is the EP gradient, the rate of increasing EP with respect to decreasing depth.

196 The electric current is the result of anodic and cathodic reactions occurring in the METland®.
197 Therefore, the analysis of electric fields recorded in an EP profile, could be used to estimate the
198 areas acting as electron sources and electron sinks along biofilter profile (Damgaard et al., 2014).
199 The electron transfer rate (*R)* can be estimated (adapted from Risgaard-Petersen et al., 2014):

200 $$(Eq.2) \qquad R = -\frac{dJ}{dz} \cdot \frac{1}{F}$$

201 Where *R* is the rate of electron transfer from reactions per unit volume [µmol m^{-3} s^{-1}], $\frac{dJ}{dz}$ is the
202 gradient of electron current density [A m^{-2} m], and *F* is the Faraday constant [9.65 x 104 C mol^{-1}].

203 ***2.5 Statistical analysis***

204 Removal efficiencies were calculated as a percentage of the total inlet concentration of pollutants.
205 Removal rates were obtained from the inlet-outlet difference as grams per cubic meter of bed per
206 day. The data in the bar graphs corresponds to the average value of 3 measurements taken once
207 steady state conditions was reached. In order to discern the true effect of the bed materials for each
208 operation condition, statistical procedures were conducted with these 3 measurements using R
209 software (R Core Team 2013) and R-commander package (Fox 2005). The standard error of the
210 mean of these measurements is included in the error bars.

211 **3. Results and discussion**

212 ***3.1 Electric potential profiles and electron currents***

213 In order to verify this new redox gradient concept, we monitored the electric potential profiles
214 along the bed. Since the METland® operates as single electrode this methodology is key; without an
215 external circuit electrical current cannot be directly measured as typically occurs with standard
216 microbial electrochemical systems (Borjas et al., 2017). This elegant method of measuring electric
217 potential (EP) to estimate derived ionic current densities was performed previously to calculate
218 current density (*J*) along the METland® bed and the rate of electrons transfer from reactions per unit
219 volume (*R*) (Ramírez-Vargas et al., 2019). Furthermore, it has also been shown that the electrical
220 potential profile is not affected by pH or the redox gradient (Damgaard et al., 2014).

EP profiles were analysed for the three biofilters (gravel (G), ec-coke (C) and ec-biochar (ecB)) at three independent sampling points (Fig. 2) when the systems reached steady state. In addition, the systems were operated under snorkel configuration with an e-sink inside the bed. The e-sink was operated under three conditions: (i) empty as a control, (ii) with aerated water and (iii) with hypochlorite (80 mM). The EP profile showed differences between the tested systems (Fig.2), indicating the impact of electrochemical electron acceptors on the flow of ions, and consequently on the flux of electrons. This behaviour was correlated with the microbial activity, in terms of the removal efficiency of pollutants for each treatment.

The up flow operation of a conventional biofilter, made of inert material like gravel, typically leads to microbial metabolism being limited by the availability of an electron acceptor. Electrons cannot travel along the inert bed so the EP depth profile of this system showed no variations at all between sampling points. In this system, oxidation and reduction reactions leading to pollutant removal are coupled both temporally and spatially (Ramírez-Vargas et al., 2019). We confirmed such behaviour in our gravel-based biofilters (Fig. 2) which acted as control, free of a vertical redox gradient. In contrast, systems made of electroconductive bed showed variations of the EP with depth due to the transfer of electrons from the microbial oxidation of pollutants. (Fig. 2). The electric potential generated by this microbial electron transfer triggered a flux of ions in the liquid phase with the same value and magnitude but in the opposite direction of the electrons thereby closing the electric circuit.

The implementation of e-sink devices hosting different electrochemical electrons acceptors generated a new redox gradient in the horizontal axis, this provides a new dimension for the EP profiles. As expected, the sampling point closest to the e-sink device (SP1), was the one most affected. The electrons generated at the bottom layers of the bed migrated towards the e-sink device instead of towards the upper top layer where oxygen is present. For this reason, the EP vertical profile in SP1 (Fig. 2) showed a lower slope, therefore behaving similarly to gravel system. In contrast, for the sampling point farthest away (SP3) from the e-sink device, showed less influence and an EP vertical profile was similar to e-sink free systems.

The electrochemical electron acceptor used in the e-sink device significantly affected the EP vertical profiles. When the redox potential of the electron acceptor was more positive, it corresponded to a higher reduction rate of the acceptor, a higher flux of electrons, and a greater

radius of influence by the e-sink device. Operating a METland® with e-sink increased the net volume of TEA available. The electron flux was then also established along the horizontal direction and, consequently, the electron flux towards the oxygen at the uppermost surface was reduced. Such differences can be observed in the EP vertical profiles when oxygen or hypochlorite were the TEA tested the e-sink device (Fig. 2). So, the higher the TEA redox potential the lower the slope for the EP vertical profile. This is consistent with the fact that hypochlorite from e-sink consume more electrons than just oxygen, so it shows higher impact in its EP vertical profile (Fig. 2). Furthermore, the impact of e-sink in EP vertical profile was stronger in those sampling points (SP1) closer to the e-sink, and weaker in those located far away (SP3). Finally, the electrically conductive material's resistance also affected the EP profiles. The lower the material's resistance, the greater the influence from the e-sink device. This increases the flux of electrons that will be diverted to the e-sink instead of the uppermost surface, what eventually increased the efficiency of the biofilters.

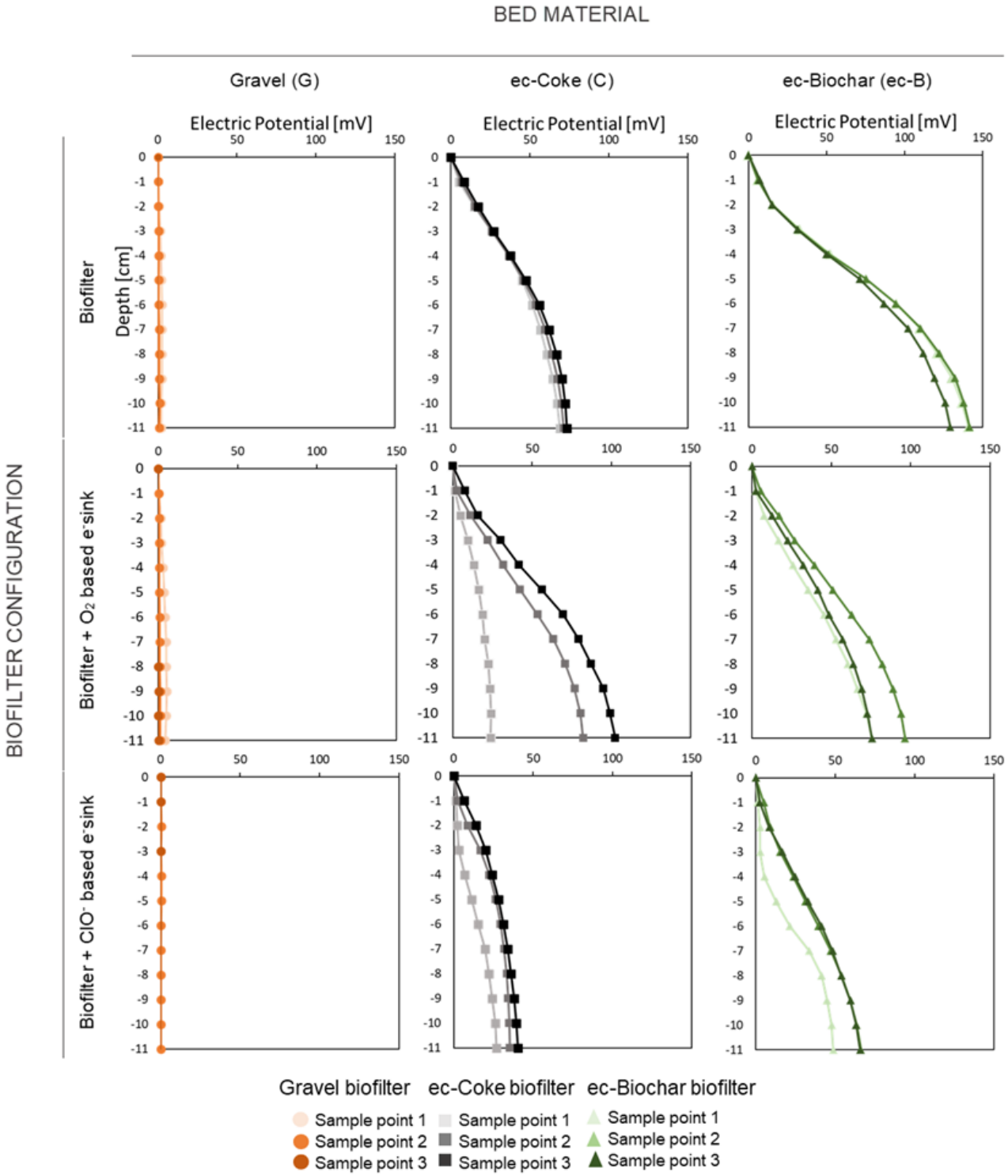

Fig. 2. Electric vertical potential (EP) profiles of tested biofilters along depth at each sampling point (SP1, SP2 and SP3) of gravel (orange), ec-coke (grey) and ec-biochar (green) bed operating as biofilter, biofilter + O_2 based e-sink and biofilter + ClO^- based e-sink. EP profiles were measured with a shielded Ag/AgCl electric potential electrode.

Our study shows that connecting microorganisms through an electrically conductive bed allows the problems associated with limited electron acceptor availability to be overcome, by coupling the

metabolism between disparate communities performing pollutant oxidation and the electrochemical reduction of electron acceptors inside the e-sink device.

As described before, METlands® represents a complete electric circuit in which charges, resulting from the organic matter oxidation by electroactive bacteria are carried as a flux of electrons through the electrically conductive bed and as ion flows through currents in the water. At steady state, these currents are equal in magnitude but opposite in direction (Damgaard et al., 2014). The ion current density *(J)* through the electrically conductive material was calculated along depth, at 1 cm interval, for each sample point (Fig. 3) in ec-coke and ec-biochar biofilters. For these calculations the *Eq. 2* was used, the values of the water conductivity are provided in Table 1S. In the gravel biofilter, it was not possible to calculate the current density since the EP at all points was not significant.

In the systems operating as standard METlands® , without an e-sink device (Fig. 3A and 3C), the profiled current density was the same at all sample points and followed the same trend in both the ec-biochar and ec-coke biofilter. The current density was increasing from the bottom layers (J= 20 mA/m^2 for ec-coke and J= 40 mA/m^2 for ec-biochar) toward the upper layers until reaching an inflection point. This point was located at 5 cm from the surface for the ec-biochar biofilter (J= 280 mA/m^2) and 3 cm from the surface for the ec-coke biofilter (J= 135 mA/cm^2). The current density decreased after the inflection. This inflection point indicated when cathodic versus anodic reactions were predominant, and may be caused by an increase in the concentration of electron acceptor or by a decrease in the electron donor (organic pollutants) at the upper layers of the biofilter.

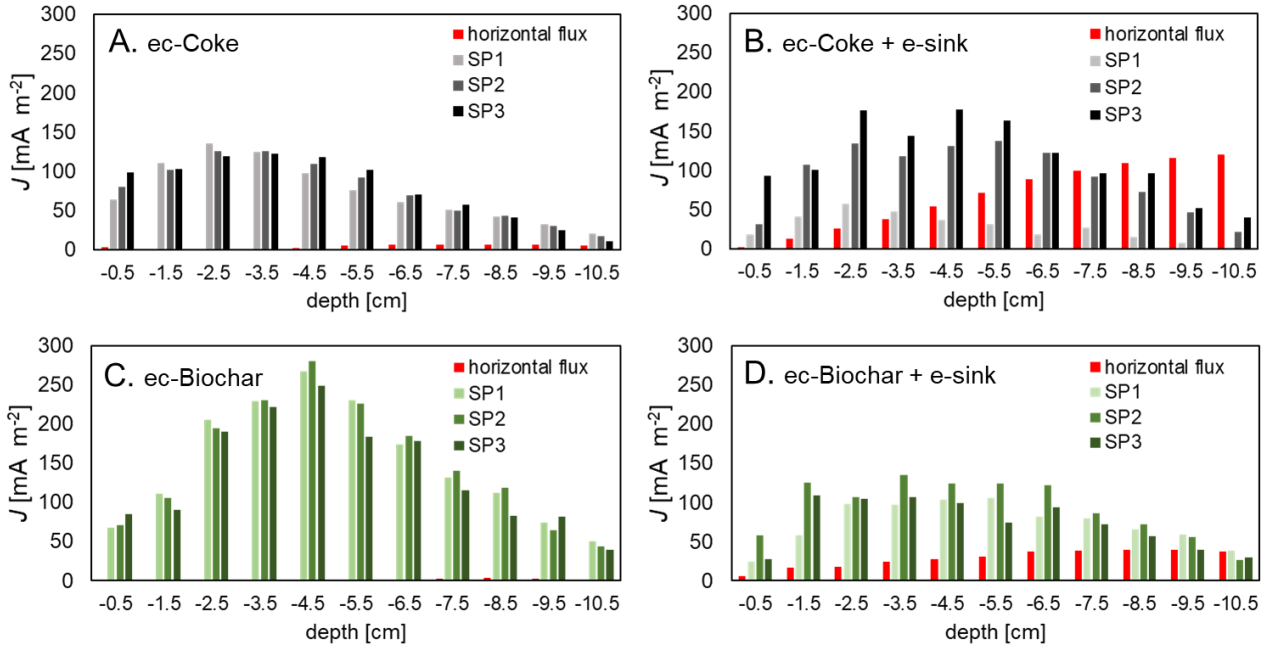

Fig. 3. Current density (*J*) values of the up-flow biofilters made of ec-coke (grey) and ec-biochar (green) in each sampling point (SP1, SP2, SP3). The systems were operated with an empty e-sink (A and C) and with an e-sink hosting oxygen saturated water (B, D). In presence of e-sink, the current density has two directions: i) vertical (grey and green bars) towards the top surface, and horizontal (red bars) towards the e-sink.

By incorporating the e-sinks into the biofilters bed the current density profile was shifted from vertical to horizontal direction (Fig. 4S). In absence of e-sink, the highest availability of TEAs was in the upper layers of the biofilter (atmospheric oxygen), so behaviour at all sample points was governed by the vertical distribution of oxygen. On the contrary, the use of a e-sink in the bed (see location in Fig. 1) add an additional redox gradient driving the flux of electrons horizontally into the e-sink. This change of direction in the flux of electrons will affect the distribution of the current density (Fig. 3B and 3D) inside the bed, including at each sampling point. The sampling point that was most affected in both ec-biofilters was SP1, as the distance between the e-sink and the SP increased, the current density was less affected. In this way, the current density profile in SP3 of both biofilters did not change (dark bars in Fig. 3B and 3D) compared to biofilters without an e-sink, which means that the entire electron flux at this sample point it went towards the uppermost surface of the biofilter. This indicates that SP3 was outside the field of influence of the e-sink. However, in SP1 (light bars in Fig. 3B and 3D), the value of *J* falls drastically compared to the values presented in the biofilters without an e-sink (Fig. 3A and 3C). Around SP1, the flux of electrons was more towards the e-sink

306 (horizontal flux). To know the value of this horizontal distribution of current density (*Eq.2*) was applied
307 to calculate *J* between SP1 and SP3 (12 cm of horizontal sampling distance). Such new distribution
308 of fluxes (red bars in Fig. 3B and 3C) revealed how the current density towards the e-sink (horizontal
309 flux) was higher at the bottom layers in both biofilters, at -11cm for both the ec-coke (120 mA / m^2)
310 and the ec-biochar (40 mA / m^2). As the distance between the e-sink TEA and the surface TEA
311 becomes similar, the current density towards the e-sink decreases (red bars in Fig. 3B and 3C) and
312 the current density towards the surface increases (light bars in Fig. 3B and 3C). The situation in SP2
313 is an intermediate state between SP1 and SP3. Beyond the physical distance to the TEA, the
314 electrical resistance of the material exerts a major influence on the distribution of the potential along
315 the bed and therefore the current density. The greater electrical conductivity of the ec-coke in
316 comparison with ec -biochar allowed a higher electronic transfer rate of the electrons towards the e-
317 sink. Therefore, the differences between current density in SP2 and SP3 were greater in the ec-coke
318 biofilter (Fig. 3B). This three-dimensional study of the current density inside a biofilter reveals how
319 the spatial location of the TEA affects the flow of charges. Still, more detailed maps are required to
320 more specifically determine the radius of influence of the e-sink.

321 The electron transfer rates (*R*) (Fig. 4) revealed the presence of electron transfer between
322 electron donors and acceptors located in different environments. Positive values signify electron
323 transfer from an electron donor (anodic reaction), while negative values signify electron transfer to
324 an electron acceptor (cathodic reaction). When the biofilters operate free of e-sink (Fig. 4) the main
325 electron acceptor will be the oxygen present in the upper layers and the main electron donor is the
326 organic pollutants supplied from the bottom. Thus, in the bottom layers the electron transfer rate was
327 positive and corresponded to areas where anodic reactions predominate, like the oxidation of organic
328 pollutants. Negative values of *R* indicate that cathodic reactions dominate over anodic reactions.
329 The reason for that could be a higher availability of TEAs, such as nitrate or oxygen, or because
330 there is less organic pollutant that can be potentially oxidized. This will also be a consequence of the
331 amount of electrons generated as a result of the oxidation processes that occurred in the bottom
332 layers, the more oxidation, the more electron flux and more electron acceptor is required. In the
333 absence of an electron acceptor, oxidation reactions and therefore the removal of the organic matter
334 will be limited. According to the electron transfer rates (*R*) (Fig. 4), the cathodic area in the ec-biochar

biofilter reaches deeper environments, up to -4 cm in absence of e-sink, while in the ec-coke biofilter it was located just two centimeters closer to the surface.

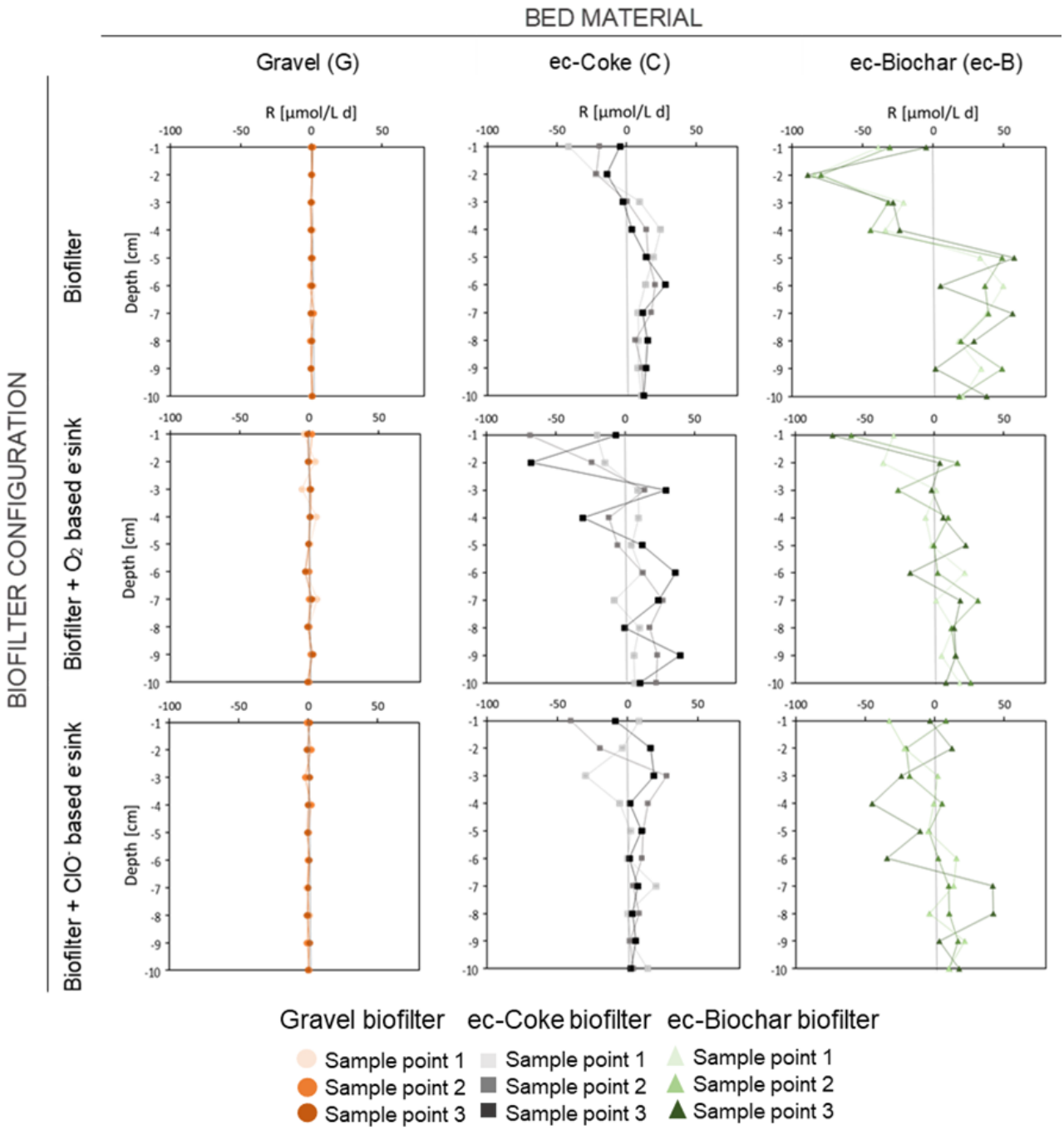

Fig. 4. Vertical distribution of electron transfer rates (*R*) for the three biofilters, gravel (orange), ec-coke (grey) and ec-biochar (green), operating without e-sink, O_2 based e-sink and ClO^- based e-sink. Positive values signify electron transfer from an electron donor (anodic reactions), while negative values signify electron transfer to an electron acceptor (cathodic reactions).

3.2 Pollutants Removal rates and electron flux

The impact of our e-sink device was evaluated with different bed materials by measuring the COD removal efficiency and the flux of electrons. The organic matter removal rates revealed different responses to reach treatment (Fig. 5).

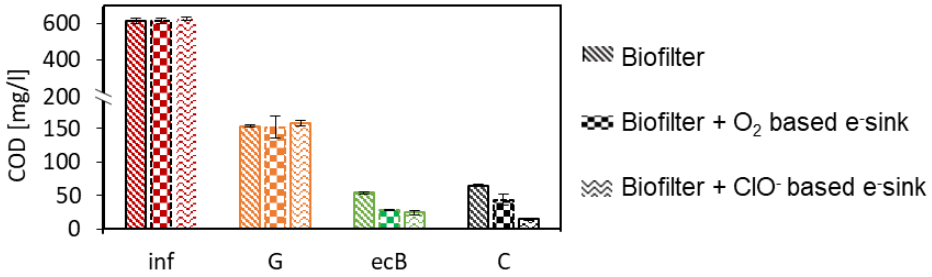

Fig. 5. COD concentration at the influent (red) and effluent of each biofilters: gravel (orange), ec-biochar (green) and ec-coke (grey), operating up flow with e-sink either in absence of electron acceptor or in presence of oxygen (O_2) and hypochlorite (ClO^-).

Table 2. Influent and effluent COD concentration, removal rate and efficiency for the different systems.

	COD Concentration [mg L^{-1}]				COD Removal rate [g/m^3 day]			COD Efficiency [%]		
Biofilter	Influent	G	ecB	C	G	ecB	C	G	ecB	C
+ e^-sink free	613.0 ± 14	153.0 ± 2	54.2 ± 2	65.1 ± 2	110.4 ± 3	134.2 ± 3	131.6 ± 4	75.0 ± 1	91.0 ± 1	89.0 ± 1
+ e^-sink (O_2)	615.0 ± 17	15.8 ± 16	28.3 ± 1	43.8 ± 8	111.0 ± 8	140.9 ± 4	137.2 ± 6	74.0 ± 3	95.0 ± 1	93.0 ± 2
+ e^-sink (ClO^-)	627.0± 10	157.0 ± 4	24.4 ± 4	14.6 ± 2	112.8 ± 3	144.7 ± 2	147.1 ± 3	74.0 ± 1	96.0 ± 1	98.0 ± 1

When biofilters without e-sinks were operated in the up flow configuration, the electron acceptor in the medium was mostly oxygen present at the surface and nitrate, resulting from the nitrification. In the case of the gravel biofilter, the oxidation processes of organic matter are very limited because the majority electron acceptors are only available at the top layer. Due to this limit in TEAs, our gravel biofilter did not have a COD removal efficiency higher than 75%. Taking into account that the influent COD was around 600 mg/L (Table 2), and the effluent COD was 150 mg/L, then the standard system did not fulfil the discharge limit (Dir. 00/60 / EC of 23 Oct 2000) for treated urban wastewater. Although the TEA concentration was increased with the e-sink, the efficiency of the gravel biofilter did not increase since these TEAs were not dissolved in the bed and could not be reduced intracellularly. Therefore, the removal efficiency remained constant around 75% operating under the three conditions (Table 2). In METlands®, electroactive bacteria can transfer electrons directly to the electrically conductive bed material therefore the flux of electrons was to the surface areas with

higher redox potential. In this way, the organic matter oxidation processes will not be slowed down despite the low availability of electron acceptor dissolved in the bed. In the ec-coke bed METland®, the COD removal efficiency was 89%. This efficiency was increased with the e-sink in the bed by increasing the effective quantity of TEA available through extracellular electron transfer and a conductive bed. Using an e-sink with oxygen saturated water, the COD removal efficiency increased to maximum of 93% and when the redox potential of the TEA is greater with hypochlorite inside the e-sink, the removal efficiency became 98% (Table 2). The effluent COD from this system is always below the discharge limit regardless of the operating condition. It should be noted that when the ec-coke METland® operates with an e-sink with hypochlorite, the COD value in the effluent is only 15 mg L^{-1} compared to 65 mg L^{-1} when it operated without an e-sink (Fig. 5). In this way, the influence of the e-sink is demonstrated in biofilters where there is an electrically conductive bed with a low internal resistance.

According to previous studies (Prado et al., 2019), the presence of carbonaceous electrically conductive materials based on pyrolyzed biomass can stimulate microbial oxidative activity more than in ec-coke beds. The ec-biochar METland® without an e-sink had a removal efficiency of 91% (Table 2). The efficiency of the system increases with an e-sink in the bed, but in this case the redox potential of the TEA did not have much influence. The effluent COD values from the ec-biochar METland® drop from 54 mg L^{-1} (without e-sink) to 28 mg L^{-1} for the e-sink with oxygen and 24 mg L^{-1}, with hypochlorite. Although the effluent COD is slightly higher than in METland® ec-coke, it always remains below the discharge limit.

These results indicate that high electron acceptor availability, whether that be direct or indirect, is a requirement for achieving higher removal rates in METlands®. The high removal of COD under a high loading rate reveals the benefits of using an electrically conductive material combined with the high availability of TEAs inside the e-sink device.

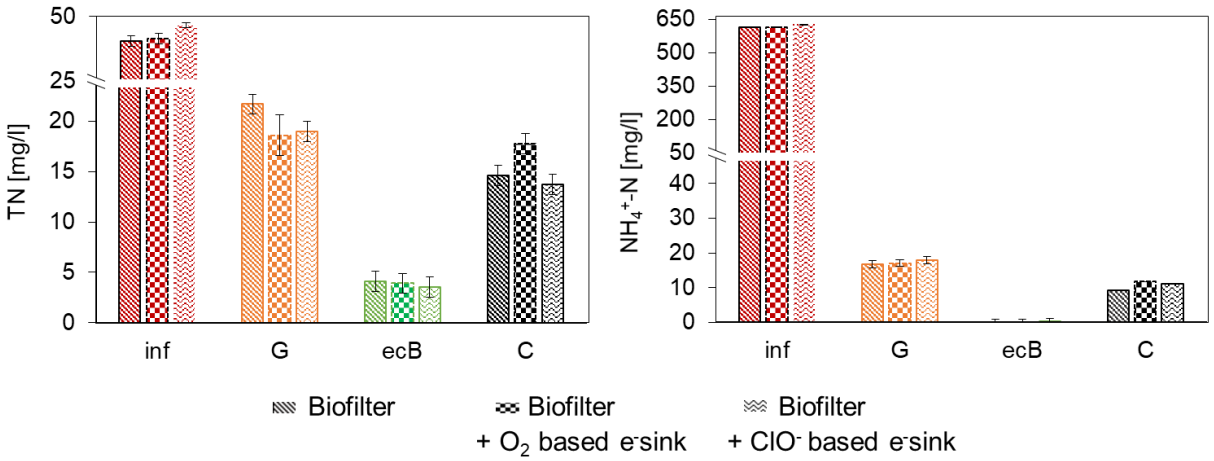

388

389 **Fig. 6.** NH_4^+-N (left) and TN (right) concentration for the three biofilters, gravel (orange), ec-coke (grey) and ec-biochar
390 (green), operating up flow with e-sink either in absence of electron acceptor or in presence of oxygen (O_2) and
391 hypochlorite (ClO^-).

392 **Table 3.** Influent and effluent NH_4^+-N and TN concentration for the different systems.

	NH4+-N Efficiency [%]			**TN Efficiency [%]**		
Biofilter	G	ecB	C	G	ecB	C
+ e-sink free	57 ± 1	100 ± 1	76 ± 1	54 ± 1	89 ± 1	64 ± 1
+ e-sink (O_2)	58 ± 1	100 ± 2	70 ± 1	55 ± 1	90 ± 2	57 ± 1
+ e-sink (ClO^-)	61 ± 1	99 ± 1	76 ± 1	69 ± 1	92 ± 1	71 ± 1

393 Nitrogen removal was studied in the three biofilters under the different e-sink conditions (Fig. 6).
394 Statistical analysis revealed significant reduction in ammonia and TN residual concentrations in the
395 effluent between gravel and electrically conductive bed biofilters. In the gravel biofilter the ammonia
396 removal efficiency was 60% and due to its non-conductive nature, such performance was not
397 affected even in the presence of the e-sink. In the ec-coke biofilter, the ammonia removal efficiency
398 was 76%, and even 100% when ec-biochar was the bed material. However, in spite of increasing
399 the COD removal, the use of the e-sink in the biofilter bed did not increase the ammonia removal
400 rate (Table 3 and Fig. 6). Such little impact of e-sink on ammonium oxidation could be due to the
401 anoxic conditions of our biological treatment in contrast with the aerobic nature of typical nitrifying
402 bacteria. In spite of the optimal ammonium removal, not all nitrate was denitrified due to the
403 competitive role of the ec-bed for accepting the electrons and to the low availiability of COD at the
404 upper layers (outlet) of the biofilter.

4. Conclusions

Our new strategy to directed the flux of electrons inside the an electroconductive bed by using an e-sink device was successful because the highest performance efficiency was achieved by the TEA solution in the e-sink with highest redox potential (Jadhav et al., 2014) (e.g., hypochlorite 1.3 V in comparison with oxygen 0.8 V). Furthermore, that the resistance of the bed material great influenced the availability of TEAs. Interestingly, the fact that the gravel bed did not exhibit any removal enhancement (Fig. 5) supports our e-sink theory that the TEAs in the e-sink remained unavailable due to the inert nature of the bed.

With this technology's great promise, there are several issues that should be further explored. For example, when scaling up what is the effective area of e-sink influence, and the cost to benefit analysis of the e-sink. Therefore, we are currently designing and integrating the e-sink into pilot and full scale METlands® to further understand their efficacy.

Declaration of Competing Interest

The authors declare that there is no conflict of interest.

Acknowledgements

This investigation received funding from the European Union's Horizon 2020 research and innovation programme under the grant agreement No. 642190 (Project "iMETLAND"; http:// www.imetland.eu) and No. 826244 (Project "ELECTRA"; http://www.electra.site). Amanda Prado de Nicolas was funded by the "Formación de Personal Investigador (FPI)" PhD fellowship programme from the University of Alcalá.

Appendix A. Supplementary data

Supplementary data to this article can be found online at…

References

Aguirre-Sierra, A., 2017. Integrating Microbial Electrochemical Systems in constructed wetlands, a new paradigm for treating wastewater in small comunities. Alcalá University, Madrid, Spain.

Aguirre-Sierra, A., Bacchetti-De Gregoris, T., Berná, A., Salas, J.J., Aragón, C., Esteve-Núñez, A., 2016. Microbial electrochemical systems outperform fixed-bed biofilters in cleaning up urban wastewater. Environ. Sci. Water Res. Technol. 2, 984–993. https://doi.org/10.1039/C6EW00172F

Aguirre-Sierra, A., Bacchetti, T., Salas, J.J., de Deus, A., Esteve-Núñez, A., 2020. A new concept in constructed wetlands: assessment of aerobic electroconductive biofilters. Environ. Sci. Water Res. Technol. 2, 984–993. https://doi.org/10.1039/c9ew00696f

Borjas, Z., Manuel, J., Esteve-Núñez, A., 2017. Strategies for merging microbial fuel cell technologies in water desalination processes: Start-up protocol and desalination efficiency assessment 1–10. https://doi.org/10.1016/j.jpowsour.2017.02.052

Brix, H., 1994. Constructed wetlands for municipal wastewater treatment in Europe. In: Mitsch, W.J. (Ed.), Global Wetlands: Old World and New 325–334. ISBN 13: 9780444814784

Brix, H., Koottatep, T., Laugesen, C.H., 2007. Wastewater treatment in tsunami affected areas of Thailand by constructed wetlands 69–74. https://doi.org/10.2166/wst.2007.528

Carleton, J.N., Grizzard, T.J., Godrej, A.N., Post, H.E., Lampe, L., Kenel, P.P., 2000. Performance of a Constructed Wetlands in Treating Urban Stormwater Runoff. Water Environ. Res. 72, 295–304. https://doi.org/https://doi.org/10.2175/106143000X137518

Corbella, C., Garfí, M., Puigagut, J., 2014. Science of the Total Environment Vertical redox pro fi les in treatment wetlands as function of hydraulic regime and macrophytes presence : Surveying the optimal scenario for microbial fuel cell implementation. Sci. Total Environ. 470–471, 754–758. https://doi.org/10.1016/j.scitotenv.2013.09.068

Damgaard, L.R., Risgaard-Petersen, N., Nielsen, L.P., 2014. Electric potential microelectrode for studies of electrobiogeophysics. J. Geophys. Res. Biogeosciences 119, 1906–1917. https://doi.org/10.1002/2014JG002665

Doherty, L., Zhao, Y., Zhao, X., Hu, Y., Hao, X., Xu, L., Liu, R., 2015. A review of a recently emerged technology: Constructed wetland – microbial fuel cells. Water Res., 85, 38-45. https://doi.org/10.1016/j.watres.2015.08.016

Dotro, G., Molle, P., Nivala, J., Puigagut, J., Stein, O., 2017. Treatment Wetlands. First. ed. IWA Publishing, London.

García, J., Rousseau, D.P.L., Morato, J., Lesage, E., Matamoros, V., Bayona, J.M., 2010. Contaminant removal processes in subsurface-flow constructed wetlands: a review. Critical Reviews in Environ. Science and Technology, 40(7), 561-661. https://doi.org/10.1080/10643380802471076

Isosaari Pirjo& Sillanpää Mika, 2016. Use of sulphate reducing bioreactors and bioelectrochemical reactors for metal recovery from mine water. Sep. Purif. Rev. 2119. https://doi.org/10.1080/15422119.2016.1156548

Jadhav, D.A., Ghadge, A.N., Mondal, D., Ghangrekar, M.M., 2014. Comparison of oxygen and hypochlorite as cathodic electron acceptor in microbial fuel cells. Bioresour. Technol. 154, 330–335. https://doi.org/10.1016/j.biortech.2013.12.069

Kadlec, R., Wallace, S., 2009. Ttreatment wetlands, in: Vasa. p. 1048. ISBN 13: 9781566705264

Nielsen, L.P., Risgaard-Petersen, N., 2014. Rethinking Sediment Biogeochemistry After the Discovery of Electric Currents. Ann. Rev. Mar. Sci. 7, 425–442. https://doi.org/10.1146/annurev-marine-010814-015708

Nielsen, L.P., Risgaard-Petersen, N., Fossing, H., Christensen, P.B., Sayama, M., 2010. Electric currents couple spatially separated biogeochemical processes in marine sediment. Nature 463, 1071–1074. https://doi.org/10.1038/nature08790

Prado, A., Berenguer, R., Esteve-Núñez, A., 2019. Electroactive biochar outperforms highly conductive carbon materials for biodegrading pollutants by enhancing microbial extracellular electron transfer. Carbon, 146, 597-609. https://doi.org/10.1016/j.carbon.2019.02.038

480 Pun, Á., Boltes, K., Letón, P., Esteve-Nuñez, A., 2019. Bioresource Technology Reports
481 Detoxification of wastewater containing pharmaceuticals using horizontal flow
482 bioelectrochemical filter. Bioresour. Technol. Reports 7, 100296.
483 https://doi.org/10.1016/j.biteb.2019.100296

484 R Core Team, 2019. R: A language and environment for statistical computing. R Foundation for
485 Statistical Computing, Vienna, Austria. https://www.R-project.org/.

486 Ramírez-Vargas, C.A., Arias, C.A., Carvalho, P., Zhang, L., Esteve-Núñez, A., Brix, H., 2019.
487 Electroactive biofilm-based constructed wetland (EABB-CW): A mesocosm-scale test of an
488 innovative setup for wastewater treatment. Sci. Total Environ. 659, 796–806.
489 https://doi.org/10.1016/j.scitotenv.2018.12.432

490 Ramírez-Vargas, C.A., Prado, A., Arias, C.A., Carvalho, P.N., Esteve-Núñez, A., Brix, H., 2018.
491 Microbial electrochemical technologies for wastewater treatment: Principles and evolution from
492 microbial fuel cells to bioelectrochemical-based constructed wetlands. Water 10(9).
493 https://doi.org/10.3390/w10091128

494 Risgaard-Petersen, N., Damgaard, L.R., Revil, A., Nielsen, L.P., 2014. Mapping electron sources
495 and sinks in a marine biogeobattery. J. Geophys. Res. G Biogeosciences 119, 1475–1486.
496 https://doi.org/10.1002/2014JG002673

497 Roley, S.S., Tank, J.L., Stephen, M.L., Johnson, L.T., Beaulieu, J.J., Witter, J.D., 2012. Floodplain
498 restoration enhances denitrification and reach-scale nitrogen removal in an agricultural stream.
499 Ecol. Appl. 22, 281–297. https://doi.org/10.1890/11-0381.1

500 Sato, M., Mooney, H.M., 1960. The electrochemical Mechanism of sulfide delf-potentials.
501 Geophysics XXV, 226–249. https://doi.org/https://doi.org/10.1190/1.1438689

502 Srivastava, P., Yadav, A.K., Abbassi, R., Garaniya, V., Lewis, T., 2018. Denitrification in a low carbon
503 environment of a constructed wetland incorporating a microbial electrolysis cell. Journal of
504 Environ. Chem. Eng., 6(4), 5602-5607. https://doi.org/10.1016/j.jece.2018.08.053

505 Vymazal, J., 2014. Constructed wetlands for treatment of industrial wastewaters : A review. Ecol.
506 Eng. 73, 724–751. https://doi.org/10.1016/j.ecoleng.2014.09.034

507 Vymazal, J., 2008. The use constructed wetlands with horizontal sub-surface flow for various types
508 of wastewater. Ecol. Eng., 35, 1–17. https://doi.org/10.1016/j.ecoleng.2008.08.016

509 Wang, Y., Zhao, Y., Xu, L., Wang, W., Doherty, L., Tang, C., 2017. Constructed wetland integrated
510 microbial fuel cell system: looking back, moving forward. Water Science and Technology,
511 76(2), 471-477. https://doi.org/10.2166/wst.2017.190

512 Wu, H., Zhang, J., Hao, H., Guo, W., Hu, Z., Liang, S., Fan, J., 2014. Bioresource Technology A
513 review on the sustainability of constructed wetlands for wastewater treatment: Design and
514 operation. Bioresour. Technol. https://doi.org/10.1016/j.biortech.2014.10.068

515 Wu, S., Kuschk, P., Brix, H., Vymazal, J., Dong, R., 2014. ScienceDirect Development of constructed
516 wetlands in performance intensifications for wastewater treatment: A nitrogen and organic
517 matter targeted review. Water Res. 57, 40–55. https://doi.org/10.1016/j.watres.2014.03.020

518 Zhao, Y., Collum, S., Phelan, M., Goodbody, T., Doherty, L., Hu, Y., 2013. Preliminary investigation
519 of constructed wetland incorporating microbial fuel cell: Batch and continuous flow trials.
520 Chem. Eng. J. 229, 364–370. https://doi.org/10.1016/j.cej.2013.06.023

521 Schievano, A., Berenguer, R., Goglio, A., Bocchi, S., Marzorati, S., Rago, L., Louro, R.O., Paquete,
522 C. M., Esteve-Núñez, A., 2019. Electroactive Biochar for Large-Scale Environmental
523 Applications of Microbial Electrochemistry. Sustainable Chem. Eng. 7, 22, 18198-18212.
524 https://doi.org/10.1021/acssuschemeng.9b04229